

## CHAPTER 2

### Theoretical Background

This chapter provides the relevant literature on the transparent conducting films. The background of the ultrasonic spray pyrolysis technique, which used film preparation in this work and the literature reviews of these films are also presented will be described.

#### 2.1 Transparent conducting films

Transparent conducting films or transparent conductive oxide (TCO) films are materials that show (1) a large energy band gap, (2) exhibit high electrical conductivity, (3) high transparency in the visible and near infrared region and (4) high reflectance in the infrared region [2]. These films are used for a wide range of transparent electrodes in many optoelectronic devices such as flat panel displays, photovoltaic cell, organic light emitting diodes, thin film transistors, smart windows and optical waveguides [5-6,8]. TCO film is suitable for these optoelectronic devices because this film is a wide band gap material greater than 3 eV with exhibit high electrical conductivity, high optical transmittance in the visible region and high reflectance in the infrared region [23]. A quantitative measure of performance of a TCO can be written in terms of the ratio of the electrical conductivity ( $\sigma$ ) to the optical absorption coefficient ( $\alpha$ ) as

$$\sigma/\alpha = 1/[R_s \ln(T+R)] \quad (2.1)$$

where  $T$  and  $R$  are transmittance and reflectance of the sample and  $R_s$  is the sheet resistance (Resistivity/film thickness) [24].

TCO films have been prepared from oxide-based materials such as  $\text{In}_2\text{O}_3$ ,  $\text{SnO}_2$ ,  $\text{CdO}$  and  $\text{ZnO}$  (Figure 2.1) [9, 11, 25]. Doping the oxide-based materials both are n-type electron semiconductors and p-type hole semiconductors with produces improved electrical conductivity without decreasing the optical transmission [9]. The difference between n-type and p-type semiconductor are described in the following section.

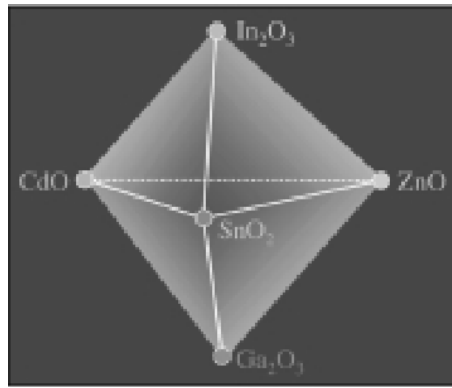


Figure 2.1 Phase space of binary oxides of TCO films [25].

### 2.1.1 P-type semiconductor

P-type semiconductor is a type of extrinsic semiconductor where the dopant impurities atoms acting as an acceptor to an intrinsic semiconductor, this addition creates deficiencies of valence electrons, called "holes" or "positive charge carrier" [26]. The most common example is atomic substitution in group IV solids (e.g. silicon (Si), germanium (Ge) and tin (Sn)) by group III elements (e.g. boron (B), aluminium (Al) and gallium (Ga)) [26].

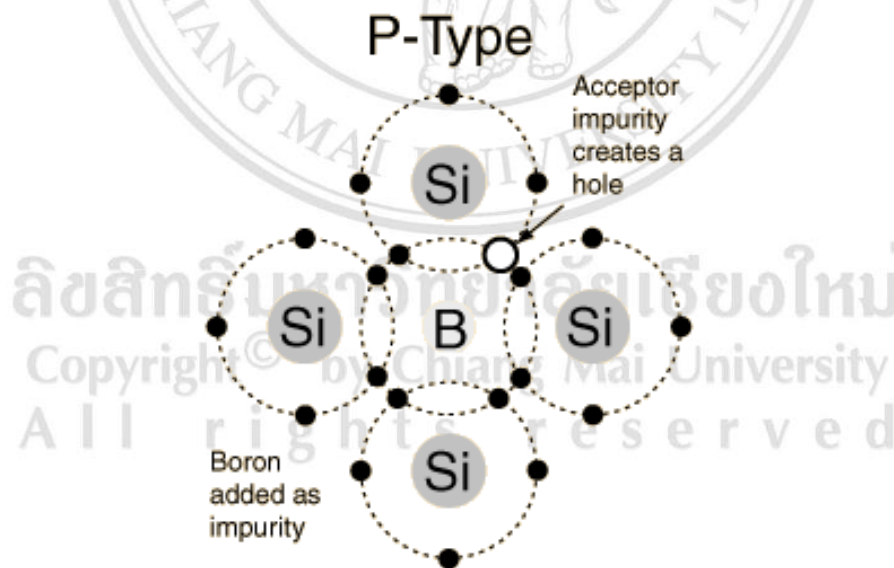


Figure 2.2 The schematic of a Si crystal lattice doped with B impurity atom [26]

For example, in silicon dioxide ( $\text{SiO}_2$ ), B atom can be created deficiencies of valence electrons (hole) when it substitutes for Si atom [26]. The

schematic of a Si crystal lattice doped with B impurity atom is shown in Figure 2.2

The impurities atoms create an acceptor band close to the valence band that is empty, the band gap decreased between a full and empty band. Therefore, electrons are able to easily jump from the valence band into the acceptor bands where they are trapped creating positive holes in the valence band, thus increasing the conductivity in semiconductor [27]. The schematic of band diagram of n-type semiconductor is shown in Figure 2.3. There are many p-type semiconductor materials were studied for TCO application such as copper aluminium oxide ( $\text{CuAlO}_2$ ), copper-scandium oxide ( $\text{CuScO}_2$ ), copper yttrium oxide ( $\text{CuYO}_2$ ), copper indium oxide ( $\text{CuInO}_2$ ), copper gallium oxide ( $\text{CuGaO}_2$ ), and copper chromium oxide ( $\text{CuCrO}_2$ ) [28].

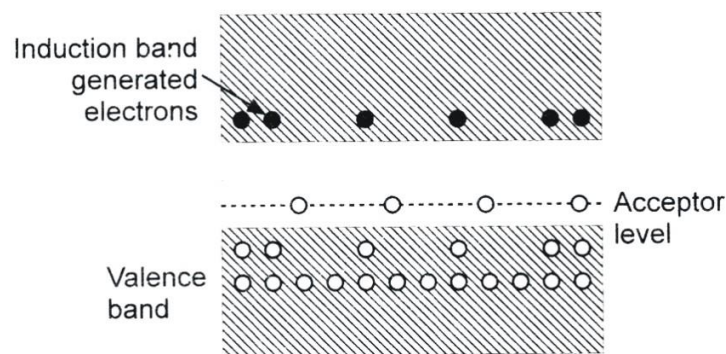


Figure 2.3 The schematic of band diagram of p-type semiconductor [29].

### 2.1.2 N-type semiconductor

N-type semiconductor is a type of extrinsic semiconductor where the dopant impurities atoms are capable of providing extra conduction electrons to the host material. This creates an excess of negative (n-type) electron charge carriers (free electron). The doping impurities atoms usually have one more valence electron than one type of the host atoms. The most common example is atomic substitution in group IV solids (e.g. silicon (Si), germanium (Ge) and tin (Sn)) by group V elements (phosphorus (P), arsenic (As) and antimony (Sb)) [30]. For example, in silicon dioxide ( $\text{SiO}_2$ ), As

atom can be a donor when it substitutes for Si atom. The schematic of a Si crystal lattice doped with As impurity atom is shown in Figure 2.4.

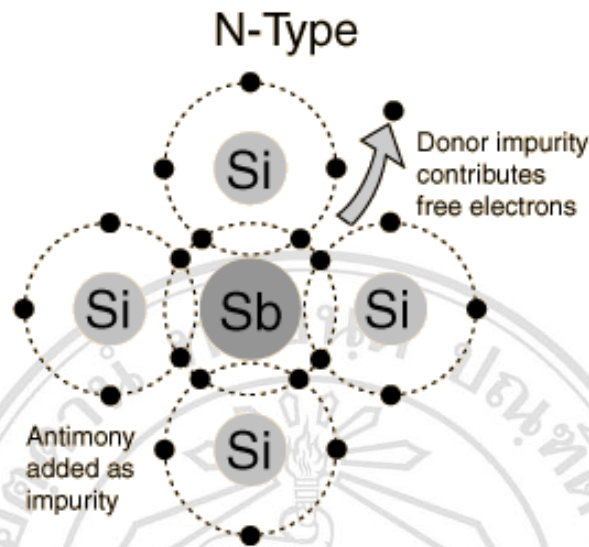


Figure 2.4 The schematic of a Si crystal lattice doped with As impurity atom [26].

This behavior increases the conductivity of semiconductor due to a donor band, which is filled with electrons. These electrons are introduced near to the conduction band in the band gap. This greatly decreases the band gap, more electrons are able to jump to the conduction band and hence a greater conductivity in semiconductor [31]. The schematic of band diagram of n-type semiconductor is shown in Figure 2.5.

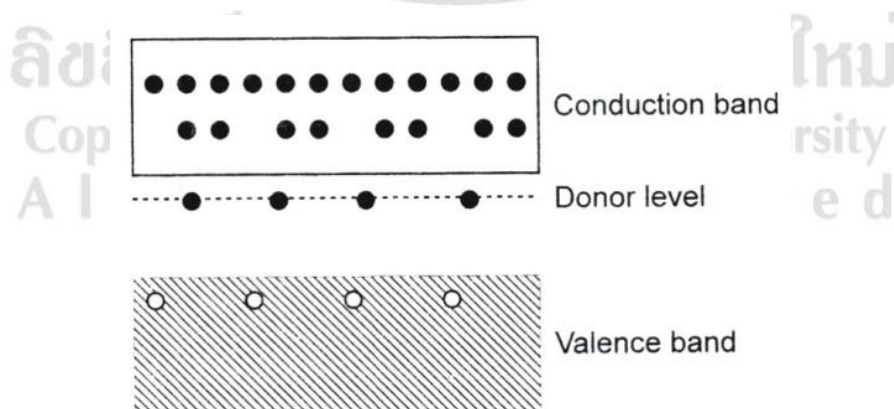


Figure 2.5 The schematic of band diagram of p-type semiconductor [29]

Most doped oxide materials are n-type electron conductors with a free electron concentration of the order of  $10^{20} \text{ cm}^{-3}$  provided by native donors

such as oxygen vacancies and/or interstitial metal atoms [9]. Example, n-type TCO films are listed in Table 2.1. However, films in CdO group is less desirable because low band gap of 2.28 eV and the toxicity of Cd [11], so n-type TCO films in In<sub>2</sub>O<sub>3</sub>, SnO<sub>2</sub> and ZnO group are widely recognized for practical applications.

Table 2.1 Type of oxide based materials, dopant elements and n-type TCO films

Oxide materials	Dopants	TCO films	Reference
In <sub>2</sub> O <sub>3</sub>	Sn	ITO	[5], [12]
	Ti	ITiO	[13]
SnO <sub>2</sub>	Sb	ATO	[14]
	F	FTO	[15], [16]
CdO	Sn	CdO: Sn	[11]
	Al	CdO: Al	[11]
ZnO	Ga	GZO	[7], [18]
	Al	AZO	[19]

## 2.2 Oxide based materials

The favorite oxide-based materials for fabrication of transparent conducting films are divided into 3 groups i.e., In<sub>2</sub>O<sub>3</sub>, SnO<sub>2</sub> and ZnO. There are many work are studied the oxide-based materials of these group, as follow.

Firstly, material of the In<sub>2</sub>O<sub>3</sub> group was been widely used as transparent conducting films in the front of ITO film. In 1999, *Benamar et al.* [5] deposited ITO film on glass substrates at 350-500°C by using spray pyrolysis and investigated physical, electrical and optical properties. Dopant concentration of 5 at.% Sn showed the lowest resistivity of about  $4 \times 10^{-5} \Omega \cdot \text{cm}$ . All films showed high transmission above 85% and the doping concentration weakly affected the transmission in the visible and near-infrared region. This research showed similar results to *El Hichou et al.* [12] where films prepared with 5 at.% Sn dopant concentration on 500°C glass substrate had lowest resistivity ( $3.3 \times 10^{-4}$

$\Omega\cdot\text{cm}$ ) and highest transmission ( $\sim 98\%$ ). Other element doped  $\text{In}_2\text{O}_3$  such as with Mg and Ti are also interesting for use as transparent conducting films. In 2008, *Moses Ezhil Raj et al.* [32] prepared Mg doped  $\text{In}_2\text{O}_3$  film on glass substrates at  $450^\circ\text{C}$  by using spray pyrolysis. It was found that the optical transmittance varied from 86-66% as the mol ratio of Mg/In was varied from 0.35 to 0.5. The electrical conductivity variations of these films, measured in the temperature range between  $30$  to  $150^\circ\text{C}$  were  $34.07 \times 10^{-5}$  to  $1.44 \times 10^{-5} \text{ S}\cdot\text{cm}^{-1}$ . In 2010, *Parthiban et al.* [13] deposited Ti doped  $\text{In}_2\text{O}_3$  Film on glass substrates at  $400^\circ\text{C}$  by using spray pyrolysis. The film doped with 2.0 at% of Ti indicated the lowest a resistivity of  $4.11 \times 10^{-4} \Omega\cdot\text{cm}$  and transmittance above 83% in the visible and near-infrared regions.

Secondly, the  $\text{SnO}_2$  group was also been widely researched and used in commercial solar cell application e.g., FTO film. In 2009, *Purushothaman et al.* [15] prepared and investigate properties of FTO film. These films were deposited on silicon wafer substrates at  $550^\circ\text{C}$  by using spray pyrolysis. The F doping concentration contributed to the decrease of resistivity up to 7.5 mol%, which had the lowest resistivity of  $15 \times 10^{-4} \Omega\cdot\text{cm}$ . In 2011, *Ren et al.* [16] fabricated FTO film with molar ratio of Sn: F = 1:0.5 on soda–lime–silica glass substrates at  $390$ - $560^\circ\text{C}$ . The sheet resistance and average transmittance of this film were  $8 \Omega/\text{sq}$  and 80.04%, respectively. Antimony (Sb) is one of the most significant dopants in tin oxide as *Shanthi et al* [14] reported in 1999. Sb doped  $\text{SnO}_2$  films were deposited on glass and quartz substrate by using spray pyrolysis. It was found that, at 9 at.% of Sb with substrate temperature of  $400^\circ\text{C}$ , the best electrical and optical properties were obtained i.e., the resistivity as low as  $9 \times 10^{-4} \Omega\cdot\text{cm}$  and average transmission of 80% in the visible region.

Finally, ZnO group is one of the most widely study for fabrication of transparent conducting films such as F doped ZnO as was reported by *Shinde et al.* [17] in 2008 results F doped ZnO films were deposited onto the corning glass substrate at  $400^\circ\text{C}$  by using spray pyrolysis and as deposited films were annealed at optimized  $200^\circ\text{C}$  for 2 hour in ambient atmosphere. The transmittance of films was in the range 80-90% in the visible region. The addition of F induced a decrease in the electrical resistivity of F doped ZnO films up to 15 at.% F doping. The lowest resistivity ( $\sim 10^{-4} \Omega\cdot\text{cm}$ ) was observed for annealed films deposited with 15 at.% F doping. Later, in 2010, *Prasada*



*Rao et al.* [18] deposited GZO films on glass substrate by using spray pyrolysis. The films were identified as polycrystalline hexagonal wurtzite type crystal structure with a preferred orientation in the (002) plane. All films showed nearly 90% transparency in the the visible region. At 3 at.% Ga doping, the film had lowest resistivity of  $6.8 \times 10^{-3}$  cm. In 2012, *Pandey et al.* [19] prepared AZO films on glass substrates at  $450^\circ\text{C}$  by using spray pyrolysis. The lowest resistivity was found at 5 at.% Al doping and films had a high level of transmission over 85% in the visible range.

In this work intends to fabricate TCO films from ITO and ZnO. The backgrounds of these materials are explained as follow.

### 2.2.1 Indium tin oxide films [33-34]

$\text{In}_2\text{O}_3$  has 2 phases of cubic (bixbyite-type) and hexagonal (corundum-type), the schematically shown in Figure 2.6. Under normal conditions, structure of  $\text{In}_2\text{O}_3$  is cubic cell with lattice constant  $10.117 \text{ \AA}$  and space group symmetry of unit cell is Ia-3. The  $\text{In}_2\text{O}_3$  has two 6-fold non-equivalents  $\text{In}^{3+}$  sites, denoted as b sites and d sites for short (Figure 2.7).

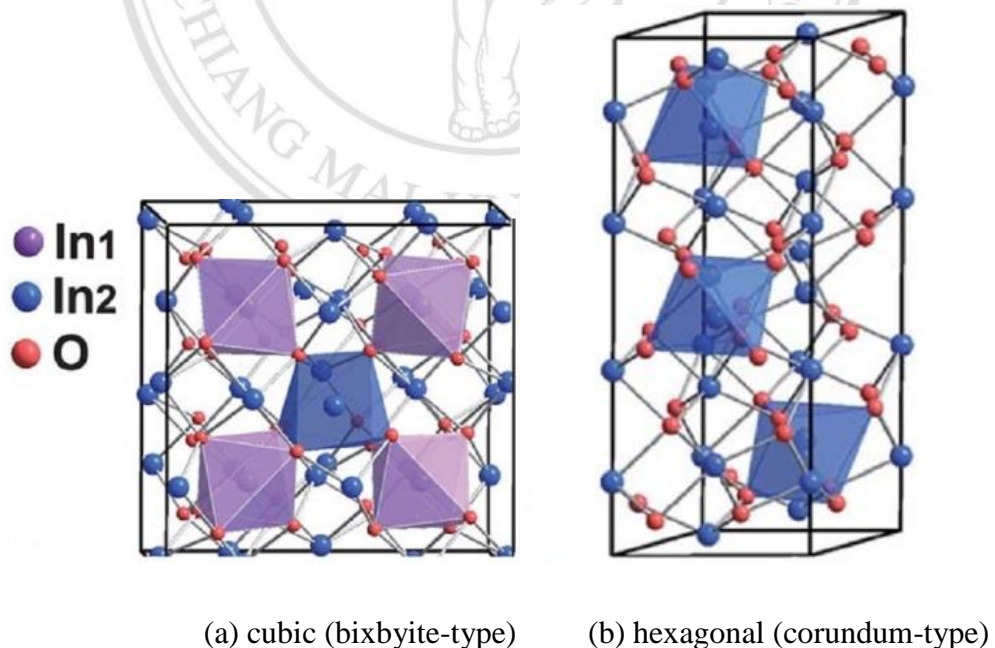


Figure 2.6  $\text{In}_2\text{O}_3$  crystal structure: cubic (bixbyite-type) (a) and hexagonal (corundum-type) (b) [35].

The b site cations have six oxygen anions neighbors, which lie at the corners of a cube with two structural vacancies along the cubic body diagonal, and these oxygen atoms are equidistant from the cations at 2.18 Å. While, the d site cations are also surrounded by six oxygen anions at distances of 2.13, 2.19 and 2.23 Å, forming a more distorted cube with two vacant anion sites along the face diagonal.

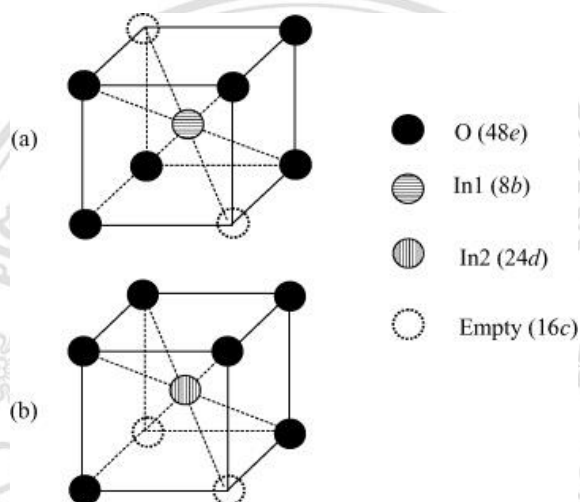


Figure 2.7 Cation sites: b site (a) and d site (b) in bixbyite type [36].

Hexagonal (corundum-type) structure is space group R-3c and the cell contains six formula units. This structure is formed under the high-pressure modification of  $\text{In}_2\text{O}_3$ , where the cations are 6-coordinated and the anions are 4-coordinated. The cations  $\text{In}_2\text{O}_3$  are in a rather regular octahedron, where the  $\text{In}^{3+}$  ions are distributed in an ordered fashion over 2/3 of the octahedral sites within a framework of hexagonally close-packed  $\text{O}^{2-}$  ions, and the cation–anion distances are 2.27 and 2.07 Å.



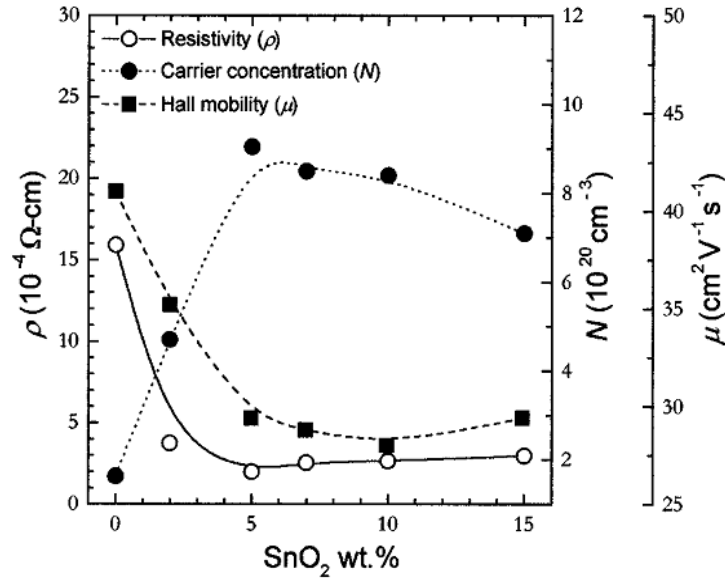


Figure 2.8 Dependence of resistivity, carrier density, and Hall mobility on SnO<sub>2</sub> content for the deposited ITO films. The substrate deposition temperature was kept at 250 °C and the oxygen pressure was 10 mTorr during deposition [37].

ITO films are modified from In<sub>2</sub>O<sub>3</sub> films by Sn doping, the Sn atom are substitute for In atom without ordering. The different of valance electron between In<sup>3+</sup> and Sn<sup>4+</sup> results in the donation of free electron to the lattice. Hence, the ITO film is high carrier density, results to exhibit low electrical resistivity (in order of 10<sup>-4</sup> Ω.cm). From the work of *Kim et al* [37], resistivity of ITO films decreased and carrier concentration increased with increasing Sn concentration, as shown in Figure 2.8. Further ITO films shows high transmittance, low absorbance and low reflectance in visible region (Figure 2.9) and a wide band gap are in the range 3.5-4.3 eV [37]

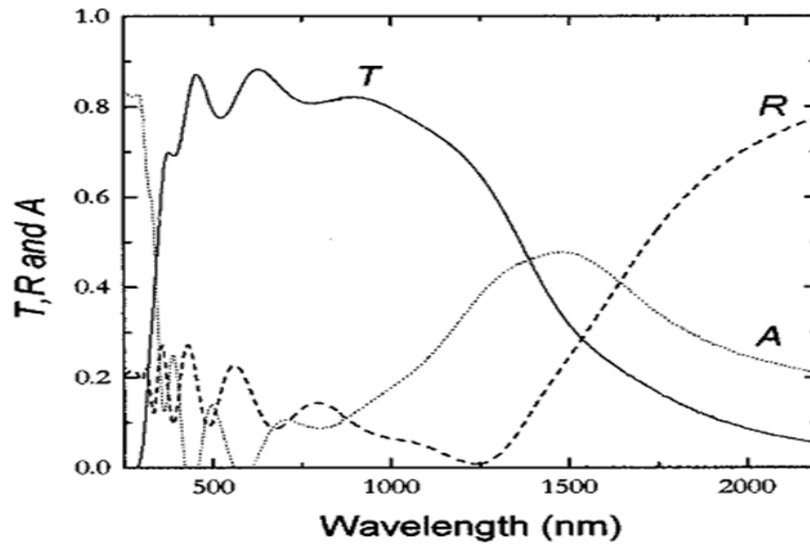


Figure 2.9 Typical transmission, reflectance, and absorption spectra for the ITO film grown at 200 °C and 10 mTorr of oxygen. The film thickness was 300 nm [37].

#### 2.2.2 Zinc oxide films [2, 38-40].

ZnO is a II–VI compound semiconductor with 3 crystal structures are wurtzite, zinc blende and rocksalt, the schematically shown in Figure 2.10. Under normal conditions, the thermodynamically stable phase is that of hexagonal wurtzite structure with space group  $C6mc$  where each anion is surrounded by four cations at the corners of a tetrahedron, and vice versa. The wurtzite structure has a hexagonal unit cell with two lattice parameters  $a = 3.25\text{\AA}$  and  $c = 5.21\text{\AA}$  with a number of alternating planes composed of tetrahedrally coordinated  $O^{2-}$  and  $Zn^{2+}$  ions attached alternately along the  $c$ -axis as shown in Figure 2.11. The oppositely charged ions produce positively charged Zn-(0001) and negatively charged O-(000 $\bar{1}$ ) surface, resulting in a normal dipole moment and spontaneous polarization along the  $c$ -axis as well as a divergence in surface energy.

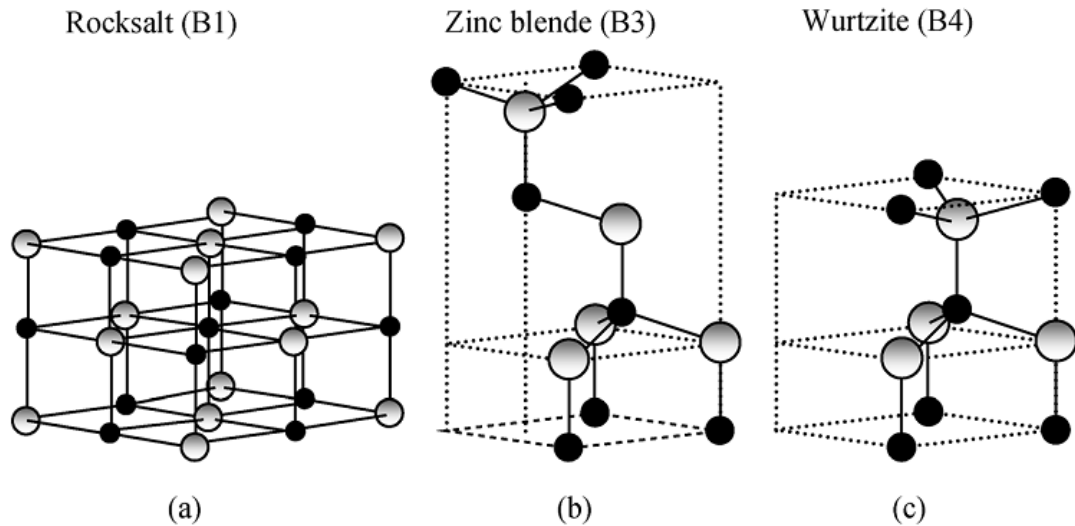


Figure 2.10 ZnO crystal structure: cubic rocksalt (a), cubic zinc blend (b) and hexagonal wurtzite (c) when shaded gray and black sphere denoted Zn and O atom, respectively [40].

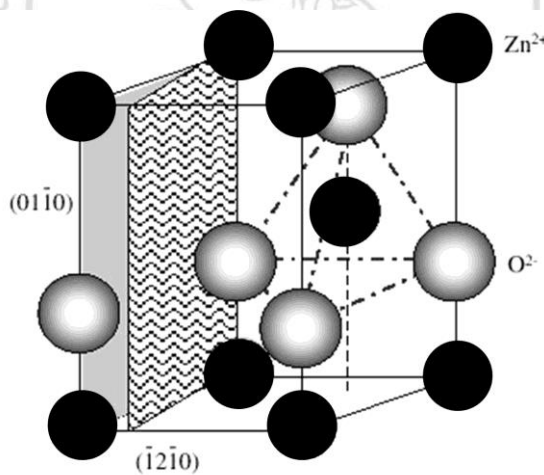
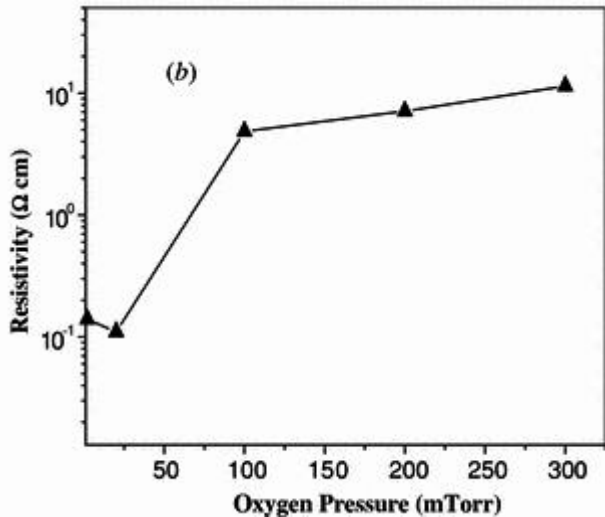
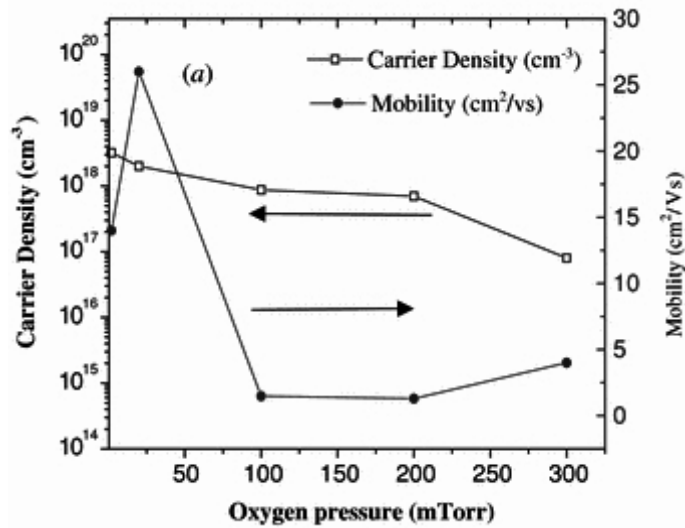


Figure 2.11 The hexagonal wurtzite structure model of ZnO. The tetrahedral coordination of Zn-O is shown [40].

Thin films of ZnO have promising electrical conductivity such as low electrical resistivity of  $10^{-4}$  -  $10^2$   $\Omega$ .cm and high carrier concentration of  $2 \times 10^{15}$  -  $1.5 \times 10^{21}$   $\text{cm}^{-3}$ . Example, carrier density, mobility and resistivity of undoped ZnO film were studied by *Li et al* (Figure 2.12) [41]. Moreover, ZnO films shows high transmittance, low absorbance and low reflectance in visible region (Figure 2.13) [42].



ลิขสิทธิ์มหาวิทยาลัยเชียงใหม่  
Copyright © by Chiang Mai University

Figure 2.12 Carrier density, mobility (a) and resistivity (b) of undoped ZnO film with different oxygen pressure [41].

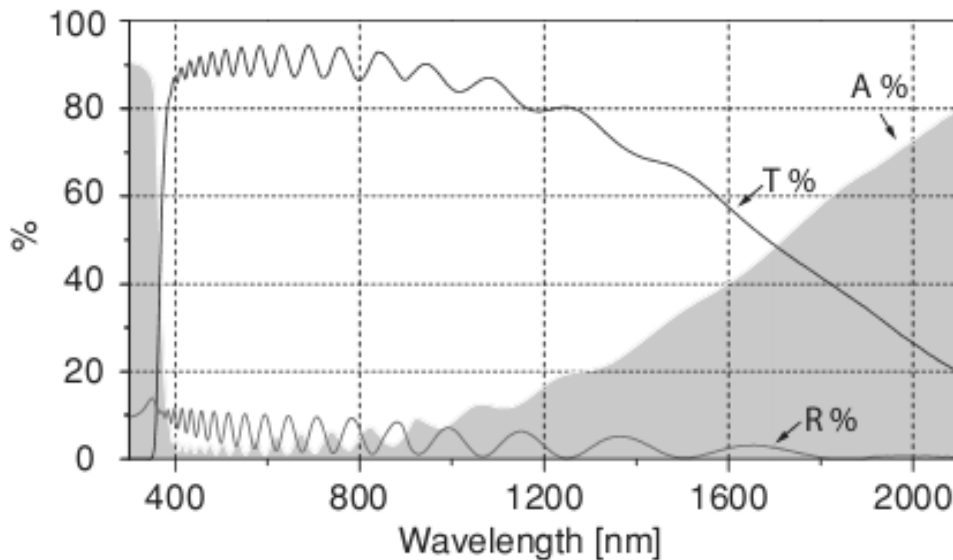


Figure 2.13 Typical transmittance, reflectance, and absorbance spectra for the Al doped ZnO film [42].

ZnO is a direct band gap semiconductor with wide band gap of 3.20 eV at room temperature. The band gap of ZnO can be tuned via divalent substitution on the cation site to produce heterostructures. Example, Cd doping can decrease the band gap to about 3.0 eV, whereas Mg doping can increase the band gap to about 4.0 eV. Electron doping in undoped ZnO has been attributed to Zn interstitials and oxygen vacancies. Most ZnO has n-type character, even in the absence of intentional doping. Controllable n-type doping is achieved by substituting ZnO with group III elements such as Al, Ga or indium (In), or by substituting oxygen with group-VII elements such as Chlorine (Cl) or iodine (I).

## 2.2 Ultrasonic spray pyrolysis

CVD, evaporation, RF and DC sputtering, sol-gel, PLD, MBE and spray pyrolysis are some preparation processes currently used to produce TCO films [20-22, 43]. The previous processes for prepared TCO films are shown in Table 2.2. The focus of this work is on TCO films for electrode of solar cells. The best technique for growth of films for this application is spray pyrolysis. Spray pyrolysis technique is a process in which a thin film is deposited by spraying a solution on a heat surface [44]. The mechanisms of

particle formation and decomposition reaction showed in Figure 2.14 [45], which is the liquid droplets (atomizer) can be produced to the particle by using pyrolysis methods. The particle was produced by evaporation of solvent, drying and pyrolysis reaction of liquid droplets inside high temperature atmosphere. Particle size and distribution depend on liquid droplets, liquid distribution, the evaporation process of solvent and material properties [44-46]. And the apparatus for prepared films by ultrasonic spray pyrolysis shows in Fig 2.15 [46]. Moreover, this technique can be used in large scale with low cost production compared to growth other films techniques [23-43]. Furthermore, this technique has the other advantage of being a continuous, chemically homogeneous and low pressure preparation [20-33].

Table 2.2 The properties of TCO films achieved by different deposition techniques [43].

Type of TCO films	Deposition techniques	% Transmittance at the wavelengths of interest	Band gap (eV)	Current concentration ( $10^{20} \text{ cm}^{-3}$ )	Mobility ( $\text{cm}^2/\text{Vs}$ )	Resistivity ( $10^{-4} \Omega.\text{cm}$ )
ITO	Commercial	*	*	*	*	1-1.9
ITO	PLD	>80	*	13.8	53.5	0.845
ITO	Spray pyrolysis	81	*	18	40	0.95
ITO	sputtering	$\geq 80$	3.78-3.80	14.6-18.9	25.7-32.7	1.28-1.29
FTO	Spray pyrolysis	$\geq 75$	4.12-4.18	1.02-9.59	11.1-18.9	*
FTO	Spray pyrolysis	*	*	24.9	6.59	3.8

\* means unavailable

Table 2.2 The properties of TCO films achieved by different deposition techniques  
(continued) [43].

Type of TCO films	Deposition techniques	% Transmittance at the wavelengths of interest	Band gap (eV)	Current concentration ( $10^{20} \text{ cm}^{-3}$ )	Mobility ( $\text{cm}^2/\text{Vs}$ )	Resistivity ( $10^{-4} \Omega.\text{cm}$ )
FTO	Spray pyrolysis	~80	3.15-3.57	4.5-7	12-24	3.85-7.51
FTO	CVD	~80	*	3.05	19	10.9
AZO	MBE	*	*	2.1	57	*
AZO	sputtering	*	*	~5.5	67	1.4
AZO	sputtering	>80	*	15	22	1.9
AZO	sputtering	>85	*	9	25	2.7
AZO	sputtering	>85	3.18-3.36	*	*	980
AZO	PLD	89-95	*	13.1	36.7	1.3
AZO	PLD	>88	*	15	47.6	0.85
AZO	PLD	75-90	3.51-3.86	20.2	16.2	1.91
GZO	MBE	>80	*	8.1	42	1.9
GZO	MBE	>90	*	3.5-15	18-40	$\geq 1.9$
GZO	CVD	>85	*	*	*	1.2
GZO	Sputtering	~90	3.37-3.43	1-6	5-35	5.3
GZO	PLD	>90	3.51	146	30.96	0.812
GZO	PLD	>90	*	64	4.9	2.6

\* means unavailable



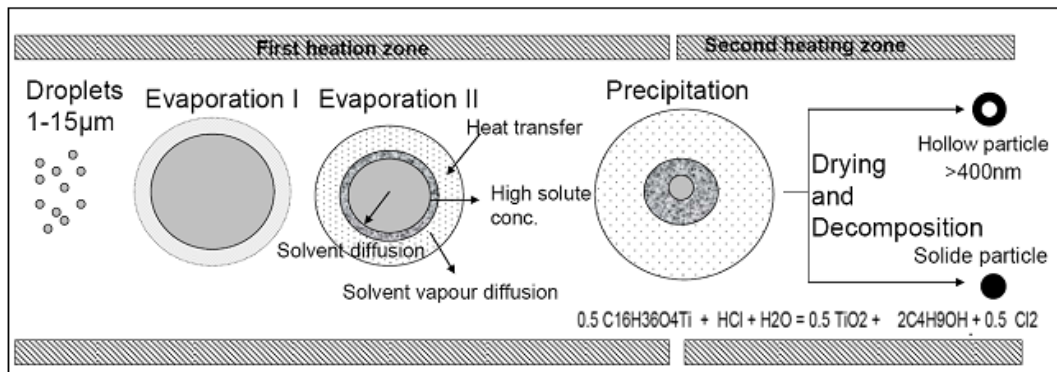


Figure 2.14 The mechanisms of particle formation and decomposition reaction [45].

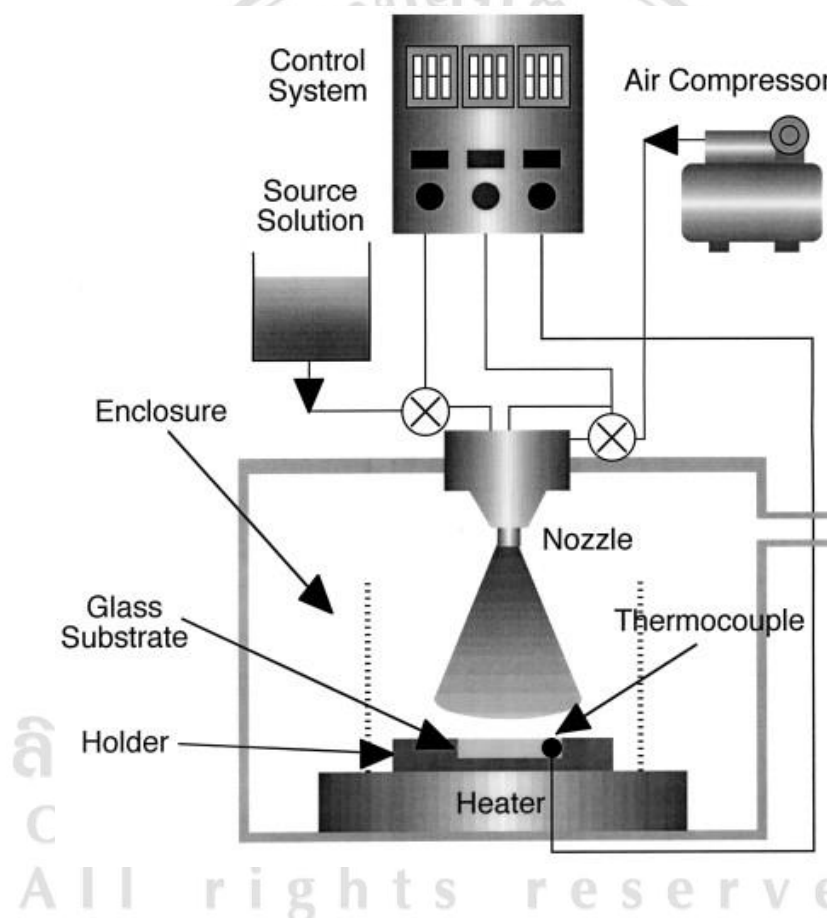


Figure 2.15 Schematic representations of spray pyrolysis deposition apparatus [46].

Modification of the spray pyrolysis technique to ultrasonic spray pyrolysis technique, the air nozzle is change to the ultrasonic frequency vibrating nozzle. This technique will be used in this work. Ultrasonic spray is created using high frequency sound vibrations (ultrasonic vibration), which are converted to mechanical vibrations. As liquid is fed through the ultrasonic nozzle, it is subjected to these mechanical vibrations [47]. The vibration of ultrasonic nozzle can be dispersed the particle into a fine atomized spray of

uniform droplet. While, air spray nozzle are low dispersion of the particle and clog easily [48]. The dispersion of particle in droplet of ultrasonic nozzle and air spray nozzle are shown in Figure 2.16. Moreover, the droplets from this nozzle can be controlled to be very small in the micron region, and smaller than from the air spray nozzle. The films can then be homogenous, without pin holes and with grain size in the nano scale [22].

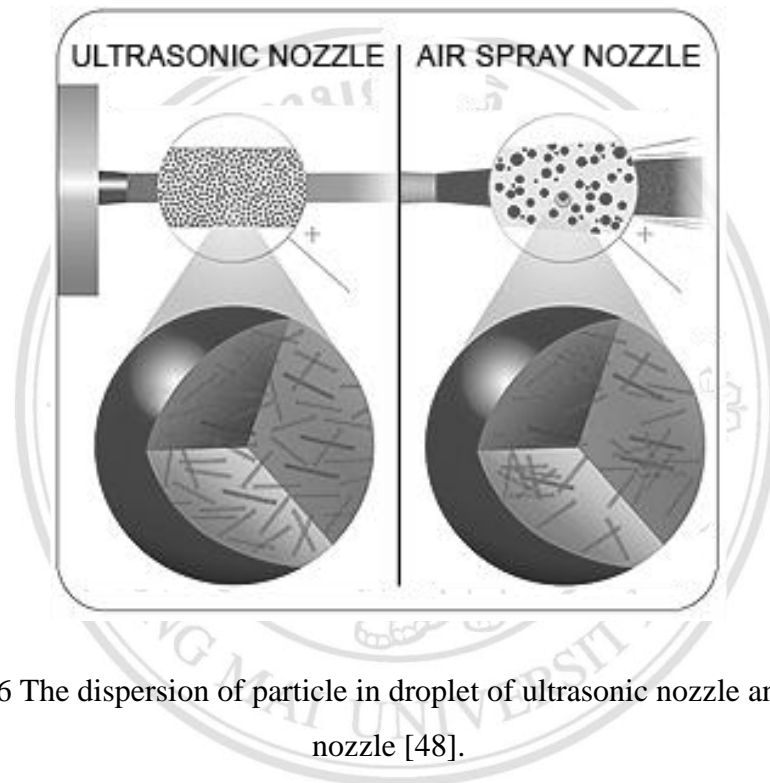


Figure 2.16 The dispersion of particle in droplet of ultrasonic nozzle and air spray nozzle [48].

## 2.3 Literature Review

### 2.3.1 Indium tin oxide

Indium tin oxide (ITO) film is n-type semiconductor and has shown low electrical resistance and high transparency in visible and near-infrared region [49]. These properties are suitable for transparent conducting film applications. The focus of this work is the preparation of transparent conducting films by using ultrasonic spray pyrolysis. Therefore, these literature reviews of this part are scope on ITO films prepared from spray pyrolysis. Firstly, ITO films were prepared by using spray pyrolysis technique and studied structural, optical and electrical properties in 1999 by

*Benamar et al* [5]. ITO films were prepared at difference Sn dopant concentration (1-10% Sn) and sprayed on microscope and Pyrex glasses heated at 350-500°C. ITO layer on Pyrex glasses heated at 500°C at 5% Sn dopant concentration showed lowest resistivity values around  $4 \times 10^{-5} \Omega \cdot \text{cm}$ . The transmittance in visible and near-infrared range of this condition is 85-90% and band gap was 3.7 eV. Later, *Rozati and Ganj* [6] investigated the effect of tin doping on physical properties of  $\text{In}_2\text{O}_3$  in 2004, In this research, the polycrystalline ITO film with difference Sn concentration of 1 to 100 wt%  $\text{SnCl}_2$  were prepared on corning 7059 glass substrate. These films showed low sheet resistance (25  $\Omega/\text{sq}$ ) and high visible transmission (~82%) were obtained when the films were deposited at Sn concentration of 2 wt%. In 2009, *Aouaj et al.* [50] investigated the comparative study of indium tin oxide and fluorine tin oxide films grown by spray pyrolysis at 400°C. The highest resistivity was  $8 \times 10^{-4} \Omega \cdot \text{cm}$  for ITO at 6%Sn.

In addition, there are many techniques tried to improve the electrical properties of TCO film. One technique to improve the electrical properties of TCO films is to use TCO/metal/TCO multilayer films, which have lower resistivity than TCO single layer films of the same thickness. The metals for practical use are silver (Ag), Au, copper (Cu) and platinum (Pt) [51-54]. This technique can be reduced the resistivity of ITO single layer films in many research. Example, the research of *Jeong et al.* [51] in 2009, the sheet resistance of ITO single layer film was 34  $\Omega/\text{sq}$ . This sheet resistance decreased to 4.4  $\Omega/\text{sq}$  by added Ag layer. Moreover, *Choi et al.* [53] report to ITO/Pt/ITO multilayer films in this year. The lowest resistivity of these films was  $3.3 \times 10^{-4} \Omega \cdot \text{cm}$ , which was lower than ITO single layer film was  $3 \times 10^{-1} \Omega \cdot \text{cm}$ . And also research of *Lee et al.* [52] reported to the resistivity of ITO single layer film is  $31.2 \times 10^{-4} \Omega \cdot \text{cm}$  and drop to  $0.56 \times 10^{-4} \Omega \cdot \text{cm}$  and  $1.51 \times 10^{-4} \Omega \cdot \text{cm}$  for ITO/Au/ITO and ITO/Cu/ITO multilayer films, respectively. The last one, the research of *Kim* in 2010, the sheet resistance of ITO single film is 130  $\Omega/\text{sq}$  decreased to 21  $\Omega/\text{sq}$  with added Au layer [54].

The objective of this work is improving the properties of ITO films for solar cell application. First, the ITO films were improved by Sn doping. Then, the best condition of the ITO film from first part was prepared to ITO/Au/ITO multilayer films for increasing electrical conductivity. The project results of these works are presented in chapter 4 and 5.

### 2.3.2 Zinc oxide

Zinc oxide (ZnO) is a semiconductor material which has high stability and light transparency in the visible region [55-56]. In addition, ZnO materials are low cost with low deposition temperature and outstanding electro-optical properties [55-56]. ZnO film has been applied to optoelectronic devices such as TCO layer in solar cells, liquid crystal displays and heat mirrors [57-58]. However, there are limitations of ZnO in some electro-optical applications due to the band gap of ZnO being not wide enough and low a carrier concentration in the conduction band [57].

From previous research, the band gap of undoped ZnO films was in the range 3.2-3.3 eV [59-60]. Example, the ZnO films were prepared by using envelope method in 2006 by *Caglar et al.* [59]. The wide band gap of ZnO films from this work is 3.28 eV. And this year, *Ashour et al.* [60], reported to ZnO films deposited by spray pyrolysis technique with different thicknesses of 100-300 nm. The band gap of these films is in the range 3.21-3.31 eV. Magnesium (Mg) is a suitable dopant for improvement of the band gap of ZnO films because MgO has a wide band gap of about 7.3 eV. Moreover the ionic radii of  $Mg^{2+}$  (0.57 Å) and  $Zn^{2+}$  (0.60 Å) are close, so films are found to be a single phase alloy over a wide range of Mg doping levels [58]. Example, report of *Huang et al.* [61], the wide band gap of ZnO films can be improved to 3.34 eV with 8 at.% Mg doping. Moreover, the wide band gap of ZnO films can be improved to more than 4.0 eV with heavy Mg doping ( $\geq 30$  at.%) as report of *Kaushal et al.* [57].

In addition, the doping of ZnO with group III elements can increase the electrical conductivity of ZnO film [62-64]. In is one of the group III

element, which has been used to doped ZnO film as a donor impurity, leading to electrical conductivity being increased [64-65]. Therefore, these literature reviews of this part are scope on ZnO films doped with In. From research of *Chen et al.* [65] in 2009, the resistivity of ZnO film was  $6.45 \times 10^2 \Omega \cdot \text{cm}$  and decreased with increasing In doping. The minimum of ZnO film of this research was  $9.74 \times 10^{-2} \Omega \cdot \text{cm}$  at 9 at.% In doping condition. While, the report of *Benouis et al.* [62] in 2010, the resistivity of undoped ZnO film was in the order of  $10^1 \Omega \cdot \text{cm}$  and decreased to the order of  $10^{-3} \Omega \cdot \text{cm}$  at 4 at.% In doping condition. Then the resistivity increased again with further concentrations. This concentration is a limitation of In concentration solubility in ZnO lattice, the remainder of In can result in impurity segregation and collected at the grain boundary [62]. Moreover, the In doping affect on the decreasing of the wide band gap of ZnO film, which was an effect of the merging of a donor level and the conduction band at high impurity density [66]. Therefore, ZnO film doped with In and Mg may be improved both of the wide band gap and the electrical property.

The objective of this work is improving the properties of ZnO films for solar cell application. First, the ZnO films were improved the wide band gap by Mg doping. Then, the best condition of Mg doped ZnO films were improved the electrical property by In doping. The project results of these works are presented in chapter 6-8.

ลิขสิทธิ์มหาวิทยาลัยเชียงใหม่  
Copyright© by Chiang Mai University  
All rights reserved